Applied Surface Science 257 (2011) 9455–9460

Contents lists available at ScienceDirect

Applied Surface Science

journal homepage: www.elsevier.com/locate/apsusc

A first-principles study of C + O reaction on NiCo(1 1 1) surface

Hongyan Liu[a,b], Riguang Zhang[a], Fangyuan Ding[a], Ruixia Yan[a], Baojun Wang[a,*], Kechang Xie[a]

[a] Key Laboratory of Coal Science and Technology of Ministry of Education and Shanxi Province, Taiyuan University of Technology, Taiyuan 030024, China
[b] College of Chemistry and Chemical Engineering, Shanxi Datong University, Datong 037009, Shanxi Province, China

ARTICLE INFO

Article history:
Received 27 February 2011
Received in revised form 6 June 2011
Accepted 6 June 2011
Available online 14 June 2011

Keywords:
C + O reaction
Alloy surface
Reaction barrier

ABSTRACT

A density-functional theory method has been conducted to investigate the association of C + O on (1 1 1) facets of ordered NiCo alloy and the results have been compared with those obtained on pure Ni(1 1 1) surface. In reaction of C + O, the favorable reaction path is that C adsorbed on HCP-1 site moves to the nearest Ni–Co bridge site, and associates with O migrating from FCC-1 site to result in CO adsorbed on the bridge site of Ni–Co. However, the reaction barrier is higher by 0.35 eV than that on pure Ni(1 1 1), which indicates that the incorporation of Co into the Ni crystal is not in favor of the reaction of carbon delimination.

1. Introduction

Catalytic reforming of CH_4 with CO_2 to produce synthesis gas has attracted increasing attention in recent years [1–7]. This process not only reduces greenhouse gas emission, but also produces synthesis gas with the ratio to unit which is more preferable feeds for some liquid fuel synthesis processes. It is well known that all VIII transition metals, except osmium, can catalyze this reaction. Because of its good activity and relatively low cost, metal Ni is selected as the catalyst in the reforming reaction. However, deactivation of Ni catalysts by carbon of coke formation is a serious problem [8,9].

Currently, bimetallic Ni-based catalysts [10–13], especially on non-noble metals incorporation into Ni crystal, are reported that they can suppress carbon depositon formation. Takanabe et al. [12] found that carbon deposition elimination on bimetallic NiCo/TiO_2 catalysts with an approximate Co/Ni ratio. Wang and co-workers [13] reported the same results on NiCo/MgO catalyst as that by Takanabe et al. [12]. However, the underlying details regarding of carbon elimination on bimetallic NiCo alloy are still unknown because of the complexity of CH_4/CO_2 reforming reaction.

Three types of carbon are formed on Ni-based catalysts in CO_2 reforming CH_4 reaction [14,15], which are (i) adsorbed, isolated, surface carbide (ii) bulk carbide, which is adsorbed carbon diffusion to bulk (iii) graphitic island, which covers the catalysts surface to make the catalysts deactivate. If adsorbed carbon is associated with O to produce CO, it will be prevented to diffuse into bulk and to build up of a graphite island [15]. It is commonly accepted that C mainly results from CH_4 dissociation, while O is from CO_2 dissociation in CO_2 reformming of CH_4 [3,16]. To the best of our knowledge, some investigations are centered on CO adsorption and dissociation on clean metal and alloy surface [17–22]. However, study on C + O reaction is scarce [23,24], even it has not been reported on NiCo(1 1 1).

In this contribution, we present a systematic study on the reaction of C associated with O atom resulting in CO on a well-characterized bulk alloy NiCo(1 1 1) surface by using density functional theory (DFT) method. Our main aim is to describe the detailed reaction mechanism, and also to elucidate the role of the reaction of C + O in carbon elimination.

2. Computational details

2.1. Methods

Density functional theory (DFT) calculations were performed using the Cambridge Sequential Total Energy Package (CASTEP) [25,26]. All calculations were conducted with the generalized gradient approximation (GGA) with the Perdew–Burke–Ernzerhof (PBE) exchange correlation functional [27]. Ionic cores were described by ultrasoft pseudopotential [28] and the Kohn–Sham one-electron states were expanded in a plane wave basis set up to a cutoff of 340 eV in order to obtain accurate energetics for all systems. A Fermi smearing of 0.1 eV was utilized and the corrected energy extrapolated to 0 K. Brillouin zone integration was approximated by a sum over special *k*-points chosen using the Monkhorst–Pack method [29], and they were set up to $5 \times 5 \times 1$. Geometries were optimized until the energy had converged to 2.0×10^{-5} eV/atom and the force

* Corresponding author. Tel.: +86 351 6018539.
E-mail addresses: wangbaojun@tyut.edu.cn, wangbaojuntyut@163.com (B. Wang).

0169-4332/$ – see front matter © 2011 Elsevier B.V. All rights reserved.
doi:10.1016/j.apsusc.2011.06.033

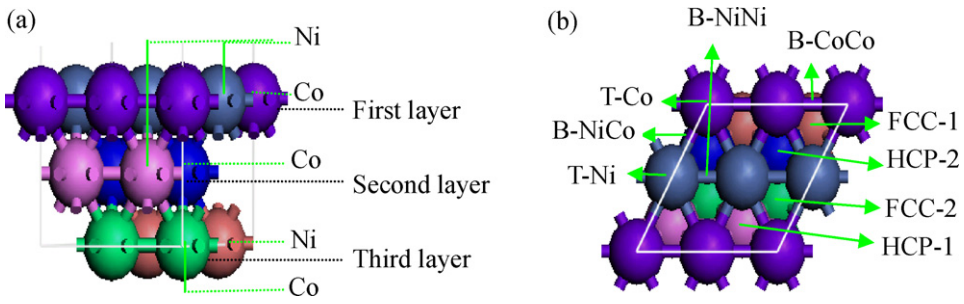

Fig. 1. The surface and adsorption sites of NiCo(1 1 1) (a) topview and (b) sideview.

converged to 0.05 eV/Å and the max displacement converged to 2×10^{-3} Å. Spin polarization was considered in all calculations.

2.2. Models

Although real catalysts feature complex surface structures, it is nevertheless useful to study the mechanism of elementary reaction steps for idealized model systems, e.g., single-crystal surfaces, if only for reference purposes. Here, we focus our investigation on (1 1 1) surface, which is the most stable.

NiCo alloy with Co/Ni ratio to unit showed the good performance in carbon dioxide reforming of methane [24]. The XRD analysis showed that uniform alloy was formed from bulk to surface. Therefore, the catalyst, including of the 1:1 Ni–Co binary system, was modeled by replacing half of the Ni atoms in a face-centered-cubic lattice by Co atoms in accordance with the structure of $L1_0$. The current calculations found a lattice constants of a is 3.511 Å, and c is 3.624 Å, which has only slight change for the lattice parameters a and c compared to the calculated lattice parameters of Ni bulk (3.541 Å) and Co bulk (3.556 Å).

The surfaces were obtained by cutting alloy of NiCo along [1 1 1] direction, the thickness of each surface slab was chosen to be at least as thick as a three layer slabs, which is proved reasonable to investigate the adsorption and reaction mechanism in previous literatures [30,31]. The vacuum region between adjacent slabs was set to 10 Å. In order to decrease the computational load, the bottom layer of slab was fixed at its equilibrium bulk phase position, while the top two layers and the adsorbates were allowed to relax freely. A (2×2) supercell was used in the calculation. Spin polarization was considered in all calculations. We restrict our attention to C and O atoms adsorbed on NiCo(1 1 1) surface, although we note that presence of subsurface C has been implicated in experiment on low index Ni surfaces.

The chemisorption energies, E_{ads}, were calculated, as follows:

$$E_{ads} = E_{adsorbates/slab} - (E_{adorbates} + E_{slab})$$

where $E_{adsorbates/slab}$ is the total energies of adsorbates on NiCo(1 1 1), $E_{adsorbates}$ is the total energy of isolated adsorbates which was calculated by putting the isolated adsorbates in a cubic box of $10 \times 10 \times 10$ Å, E_{slab} is the total energy of NiCo(1 1 1) slab.

The reaction energy was calculated by definition given as follows:

$$\Delta E = E_{A+B/slab} - E_{AB/slab}$$

where $E_{A+B/slab}$ is the total energy of the coadsorption A and B on NiCo(1 1 1) surface, $E_{AB/slab}$ are the total energies of adsorbates AB on NiCo(1 1 1) surface. For reaction $C + O \rightarrow CO$, the positive value suggests exothermic, while the negative value suggests endothermic.

Transition states (TS) are located by using the complete LST/QST method [32]. Firstly, the linear synchronous transit (LST) maximization was performed followed by an energy minimization in directions conjugate to the reaction pathway. The TS approximation obtained in that way is used to perform quadratic synchronous transit (QST) maximization. From that point, another conjugate gradient minimization is performed. The cycle is repeated until a stationary point is located. The convergence criterion for transition state calculations was set to: root-mean-square forces on atoms tolerance of 0.25 eV/Å.

The activation energy is defined as follows:

$$E_a = E_{TS} - E_R$$

where E_{TS} is the energy of transition state, and E_R is the sum of the energies of reactants.

3. Results and discussion

3.1. Adsorption of C, O and CO on NiCo(1 1 1)

There are four high symmetry sites on the (1 1 1) surface of pure Ni: top (T), bridge (B), hexagonal-close-packed (HCP) and face-centered-cubic (FCC) threefold hollow sites. On the NiCo(1 1 1) surface, some additional sites are found because of the replacement of 50% Ni atoms by Co. These adsorption sites are presented in Fig. 1. It is clearly that each group of the T, HCP and FCC sites is split into two subsets, while B sites are split into three subsets.

We first investigate the adsorption of each species involving of C + O reaction on NiCo(1 1 1). In each subsection, the adsorption of the C, O and CO is discussed and the geometries and adsorption energies are presented in Fig. 2. In addition, we calculate the adsorption of C, O and CO as well as the reaction mechanism of C + O on pure Ni(1 1 1) in order to compare the results on the two surfaces.

3.1.1. C adsorption on NiCo(1 1 1)

We have investigated the possible adsorption sites of C on NiCo(1 1 1) surface previously [33]. Herein, we collect and cite the adsorption energy of stable adsorption site and the configuration, as shown in Fig. 2. The adsorption order is as follows: HCP-1 > HCP-2 > FCC-1 > FCC-2. Our calculated adsorption energies of C on pure Ni(1 1 1) are −6.90 eV on HCP and −6.80 eV on FCC, which is higher than those on corresponding adsorption sites on NiCo(1 1 1), indicating that the addition of Co decreases the adsorption energy of C.

3.1.2. O adsorption on NiCo(1 1 1)

For O adsorption on NiCo(1 1 1), it is similar with C adsorption on NiCo(1 1 1) surface. O also preferably adsorbs on threefold sites. Their geometries are also of C_{2v} symmetry. For O on FCC-1 site, the bond of O–Ni is elongated to 1.880 Å, the bond of O–Co is elongated to 1.875 Å, and the adsorption energy is −6.01 eV. Other three adsorption energies are −5.74 eV on FCC-2, −5.97 eV on HCP-1, and −5.76 eV on HCP-2, respectively. The adsorption order is as follows: FCC-1 > HCP-1 > HCP-2 > FCC-2. Our calculated adsorption energies of O on pure Ni(1 1 1) are −5.72 eV on HCP and −5.81 eV on FCC

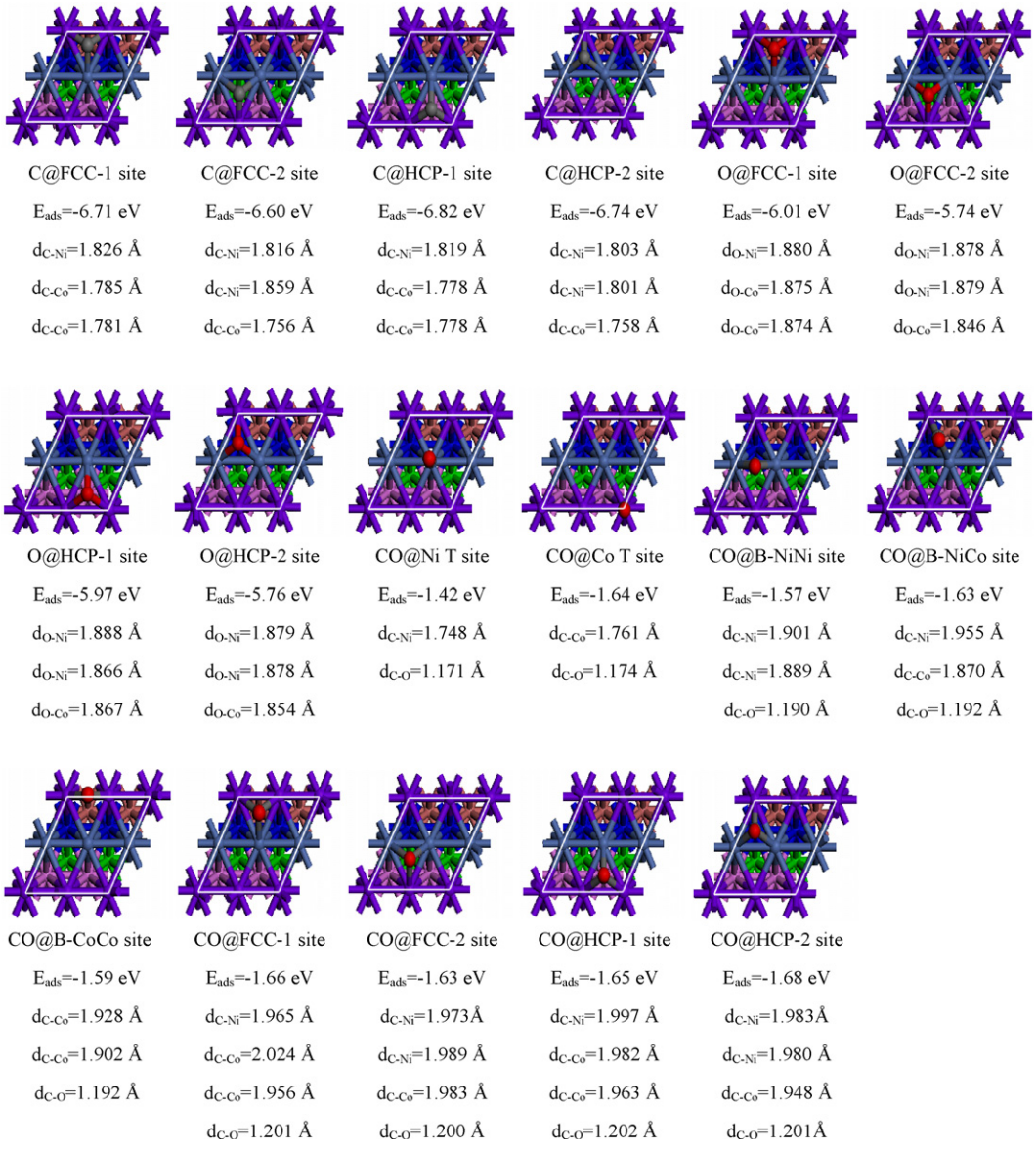

Fig. 2. The adsorption geometries and parameters of C, O and CO on NiCo(1 1 1).

site, indicating that the addition of Co affects the adsorption energy of O.

3.1.3. CO adsorption on NiCo(1 1 1)

As for CO adsorption on top sites, there are two configurations found. When CO adsorbed on the top of Ni, bound through the carbon atom to Ni atom on the NiCo(1 1 1) surface, as shown in Fig. 2. The molecular axis is perpendicular to the NiCo surface. The calculated adsorption energy is −1.42 eV, the distance of C–Ni is 1.748 Å, and the bond length of C–O is 1.171 Å. When CO adsorbed on the top of Co, there are d_{C-O} of 1.174 Å and d_{C-Co} of 1.761 Å, and the adsorption energy is −1.64 eV.

When CO is adsorbed on bridge sites, three stable configurations are found, that is, CO adsorbed on B–NiNi, B–NiCo, and B–CoCo site. The adsorption energies are −1.57, −1.68 and −1.64 eV, respectively.

There are four stable configurations obtained for CO adsorbed on threefold hollow site. On HCP-2 and FCC-2 sites, CO interacts with two Ni atoms and one Co atom, and their adsorption energies are −1.68 and −1.63 eV, respectively, while CO is bonded to two Co atoms and one Ni atom on HCP-1 (FCC-1), and the adsorption energy is −1.65 eV (−1.66 eV). The stable order for all configurations is as follows: HCP-2 > FCC-1 > HCP-1 > FCC-2. Our calculated adsorption energies of CO at FCC and HCP sites on pure Ni(1 1 1) are −1.86 and −1.84 eV, respectively, approximately equal, which indicates that the addition of Co decreases the adsorption energy of CO.

3.1.4. Electronic properties of C, O and CO

In order to profound insight into the electronic structures of the chemisorbed C, O and CO on NiCo(1 1 1), the Mulliken charges and the local density of states (LDOS) of species on HCP-1 site are shown in Table 1 and Fig. 3.

Table 1
The Mulliken charges of C, O and CO on pure Ni(1 1 1) and NiCo(1 1 1).

	C	O	CO
On pure Ni(1 1 1)	−0.45	−0.54	−0.40
On NiCo(1 1 1)	−0.46	−0.57	−0.44

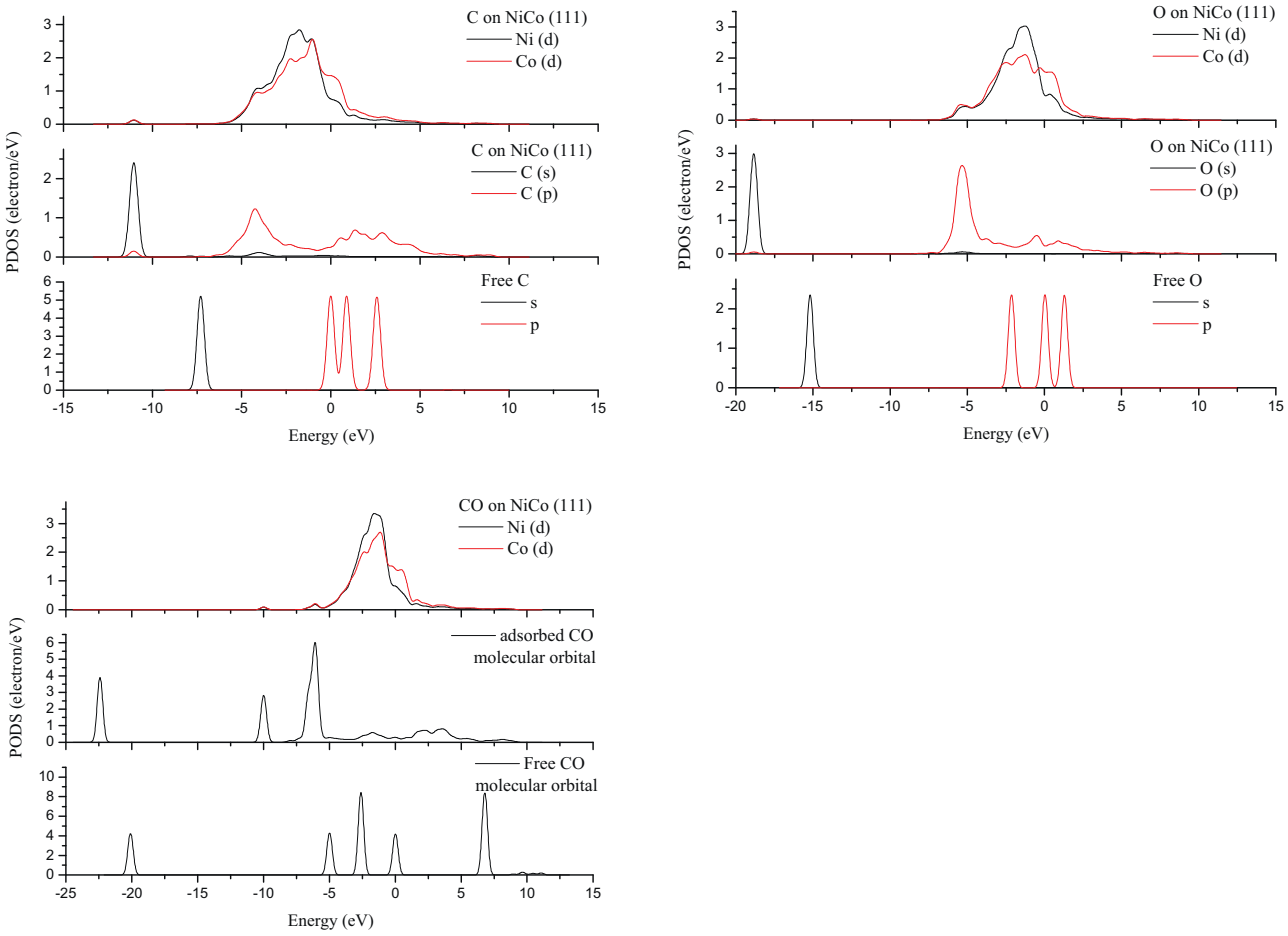

Fig. 3. The LDOS of C, O and CO on NiCo(1 1 1) and on pure Ni(1 1 1).

From Table 1, the Mulliken charges of C, O and CO adsorbed on pure Ni(1 1 1) and NiCo(1 1 1) are both negative, indicating the electron transfer from alloy NiCo surface to C, O and CO upon chemisorption, in agreement with the following LDOS analysis. Similar to those on Ni(1 1 1), the adsorbates are best described as anions. Wang et al. [31] explained that the change from free CH_x to chemisorbed $CH_x^{\delta-}$ anions makes CH_x prefer to sit on threefold hollow site because of significant charges transfer from Ni surfaces

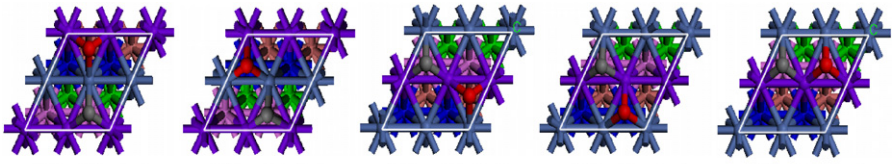

C/O **Mode 1**	C/O **Mode 2**	C/O **Mode 3**	C/O **Mode 4**	C/O **Mode 5**
E_{ads}=-12.25 eV	E_{ads}=-11.64 eV	E_{ads}=-12.25 eV	E_{ads}=-11.64 eV	E_{ads}=-11.78 eV
$\triangle E_{ads}$[a]=0.58 eV	$\triangle E_{ads}$=0.94 eV	$\triangle E_{ads}$=0.58 eV	$\triangle E_{ads}$=0.94 eV	$\triangle E_{ads}$=1.01 eV
$\triangle E_{ads}$'[b]=0.19 eV	$\triangle E_{ads}$'=0.47 eV	$\triangle E_{ads}$'=0.19 eV	$\triangle E_{ads}$'=0.47 eV	$\triangle E_{ads}$'=0.51 eV
$d_{C\text{-}Co}$=1.753 Å	$d_{C\text{-}Co}$=1.807 Å	$d_{C\text{-}Co}$=1.754 Å	$d_{C\text{-}Co}$=1.808 Å	$d_{C\text{-}Co}$=1.797 Å
$d_{C\text{-}Co}$=1.755 Å	$d_{C\text{-}Co}$=1.749 Å	$d_{C\text{-}Co}$=1.756 Å	$d_{C\text{-}Co}$=1.749 Å	$d_{C\text{-}Co}$=1.800 Å
$d_{C\text{-}Ni}$=1.811 Å	$d_{C\text{-}Ni}$=1.838 Å	$d_{C\text{-}Ni}$=1.810 Å	$d_{C\text{-}Ni}$=1.836 Å	$d_{C\text{-}Ni}$=1.791 Å
$d_{O\text{-}Ni}$=1.864 Å	$d_{O\text{-}Ni}$=1.871 Å	$d_{O\text{-}Ni}$=1.865 Å	$d_{O\text{-}Ni}$=1.863 Å	$d_{O\text{-}Ni}$=1.848 Å
$d_{O\text{-}Co}$=1.836 Å	$d_{O\text{-}Ni}$=1.862 Å	$d_{O\text{-}Co}$=1.835 Å	$d_{O\text{-}Ni}$=1.871 Å	$d_{O\text{-}Co}$=1.850Å
$d_{O\text{-}Co}$=1.834 Å	$d_{O\text{-}Co}$=1.855 Å	$d_{O\text{-}Co}$=1.835 Å	$d_{O\text{-}Co}$=1.859 Å	$d_{O\text{-}Co}$=1.851 Å
$d_{C\text{-}O}$= 2.930 Å	$d_{C\text{-}O}$= 2.555Å	$d_{C\text{-}O}$= 2.889Å	$d_{C\text{-}O}$= 2.499Å	$d_{C\text{-}O}$=2.481 Å

Fig. 4. The optimized geometries of coadsorbed C and O on NiCo(1 1 1). (a) $\Delta E_{ads} = E_{ads}(C/O) - E_{ads}(C) - E_{ads}(O)$. (b) $\Delta E'_{ads}$ is corrected energies; $\Delta E'_{ads} = \Delta E_{ads}/3$ (**Modes 1**, **3**), $\Delta E'_{ads} = \Delta E_{ads/2}$ (**Modes 2**, **4**, and **5**).

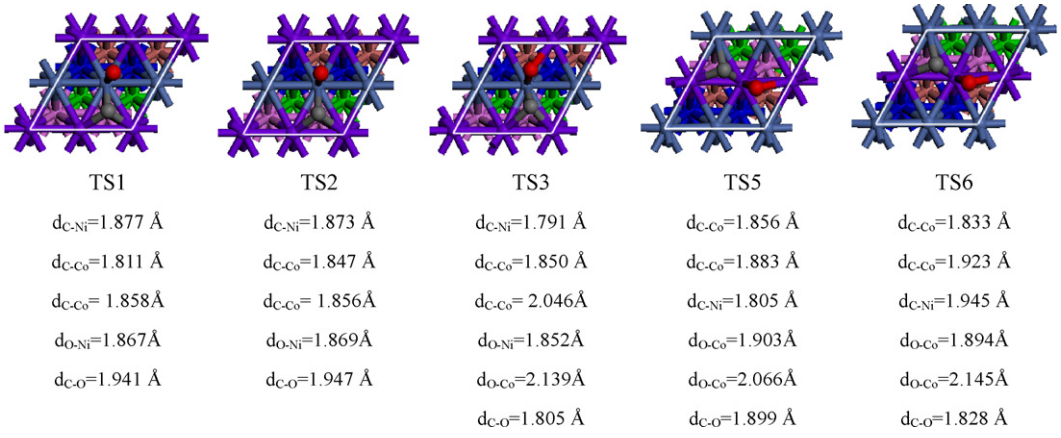

Fig. 5. Optimized structures of the transition states of C + O reaction on NiCo(1 1 1).

to CH_x upon chemisorption. Therefore, species of C, O and CO also prefer to reside on threefold hollow site on NiCo(1 1 1), which is consistent with the above results from adsorption energy.

Furthermore, we plotted the LDOS of the system projected on the orbitals for the free and adsorbed C, O and CO, as well as the NiCo substrate, as shown in Fig. 3. Fig. 3(a) and (b) displays the PDOS projected onto the free and adsorbed C(O) molecular orbitals in the NiCo(1 1 1) system. When C(O) adsorbed on NiCo(1 1 1), *s* and *p* orbitals are mixed and downshift with respect to those of free C(O), indicating interaction of *s* and *p* MO from C(O) with the substrate. This is the evidence that the presence of common peaks in the C(O) and NiCo PDOS suggests strong mixing of the two sets of electronic states with the characteristics of extraordinary hybridation. In Fig. 3(c), when CO adsorbed on NiCo alloy substrate, orbitals hybridation also occur. It is noted there is orbital broadening at the stage of species adsorbed on NiCo substrate suggesting strong bond formed in the process of adsorption. Obviously, the order of orbital broadening is as follows: C > O > CO, which is consistent with the order of adsorption energies.

3.2. C + O reaction on NiCo(1 1 1)

3.2.1. Coadsorption of C and O

In order to investigate C + O reaction on NiCo(1 1 1) surface, it is necessary to investigate the coadsorption of C and O firstly. Because C atom adsorption is stronger than O atom adsorption on NiCo(1 1 1), we only consider that C preadsorbs on the HCP-1 site, and O coadsorbs at all possible threefold sites.

Five coadsorption structures of C and O are found. The coadsorption energies and calculated bond parameters are present in Fig. 4. In coadsorption **Mode 1**(**3**), C resides at the HCP-1 site while O resides at the FCC-1 site, and they share one Ni(Co) atom in a linear way. In **Mode 2**(**4**), C resides at the HCP-1 site while O resides at the HCP-2 site, and they share one Ni(Co) in a zigzag way. C and O both reside at the HCP-1 site in **Mode 5**, and they share one Co atom in a zigzag way.

To elucidate the lateral interaction arising from coadsorption of C and O, it is necessary to value the difference (ΔE_{ads}) in adsorption energies between C and O coadsorption [E_{ads}(C/O), with respect to atomic C and O] and the sum of C and O individual adsorptions on the same site as in coadsorption [E_{ads}(C) + E_{ads}(O)]. The positive energy differences indicate that there are repulsive interactions between the adsorbed C and O atoms. From the data of ΔE_{ads} as shown in Fig. 4, it is clear that there are strong repulsive interactions between C and O in the coadsorption modes. It is well known that in the periodic slab model, the repulsion of each C(O) received from three O(C) occupied its neighboring sites in **Mode 1**(**3**), and it from two O(C) in **Mode 2**(**4** or **5**). In fact, the repulsive interaction ($\Delta E'_{ads}$) should be $\Delta E_{ads}/3$ between C and O in a unit cell in **Mode 1**(**3**), while it is $\Delta E_{ads}/2$ in **Mode 2**(**4** or **5**). Clearly, there are strong repulsion between C and O in a unit cell in coadsorption **Modes 2**, **4** and **5**, namely, they are unstable, and should be deleted in the following investigation.

Therefore, we only considered coadsorption configurations in **Modes 1** and **3** as the initial states (IS) of C + O reaction on NiCo(1 1 1). The final states (FS) consist of CO adsorbed on T–Co (or T–Ni), B–Ni–Co and HCP-1 site according to the corresponding IS configuration, respectively.

3.2.2. TS of C + O reaction

At first, the aforementioned expression of activation energy should be corrected due to repulsive interaction between C and O in a unit cell in coadsorption **Modes 1** and **3**, as follows:

$$E_a = E_{TS} - E_R - 2\,\Delta E'_{ads}$$

C + O reaction is examined. Six possible paths are mapped out (shown in Table 2). The geometries and paramenters of all possible transition states are present in Fig. 5.

Path 1 is that coadsorbed C and O in **Mode 1** combinates to produce CO adsorbed on HCP-1 site via TS1 along with O moving through the top of Ni to combinate with C adsorbed at HCP-1 site, and the distance of C–O is shortened from 2.930 Å in IS to 1.941 Å

Table 2
The reaction barriers (E_a, eV), reaction energies (ΔE, eV) of C + O reaction on NiCo(1 1 1).

Reaction path			E_a	ΔE
C + O → CO	**Path 1**	C + O(Mode **1**) → TS1 → CO(HCP-1)	1.94(1.56)[a]	−1.55(−1.17)
	Path 2	C + O(Mode **1**) → TS2 → CO(B–NiCo)	1.94(1.56)	−1.53(−1.15)
	Path 3	C + O(Mode **1**) → TS3 → CO(T–Ni)	1.82(1.44)	−1.31(−0.93)
	Path 4	C + O(Mode **3**) → TS4 → CO(HCP-1)	–	–
	Path 5	C + O(Mode **3**) → TS5 → CO(B–NiCo)	1.59(1.21)	−1.53(−1.15)
	Path 6	C + O(Mode **3**) → TS6 → CO(T–Co)	1.73(1.35)	−1.54(−1.16)

[a] Values in parentheses are corrected energies. E_a(correction) = $E_a - 2\Delta E'_{ads}$; ΔE(correction) = $\Delta E - 2\Delta E'_{ads}$.

in TS, to 1.202 Å in FS. The activation barrier is 1.56 eV and the reaction is found to be exothermic by 1.17 eV. In **Path 2(5)**, O moves through the top of Ni(Co) to the bridge of Ni–Co while C leaves its original site and moves to the bridge of Ni–Co, then O combinates with C to CO adsorbed with C end on the bridge site of Ni–Co. The distance of C–O is shortened to 1.947(1.899) Å in TS2(5). This step is exothermic by 1.15(1.15) eV with activation barrier of 1.56(1.21) eV. **Path 3(6)** is that C + O reaction via TS3(6) along with both C and O moving to the top of the same Ni(Co) to combinate producing CO adsorbed at top site of Ni(Co). The distance of C–O is shortened to 1.805(1.828) Å in TS3(6). The reaction energy and activation barriers are −0.93(−1.16) eV and 1.44(1.35) eV, respectively. There is no transition state found in **Path 4**, maybe, it is difficult for O to move through the top of Co atom. The energy data in Table 2 clearly show that all reation paths are exothermic, indicating favorable in thermodynamic. In dynamics, **Path 5** has the lowest reaction barrier, which is the most probable minimum energy path for the reaction of C + O resulting in CO on NiCo(1 1 1). However, the activation energy is higher by 0.35 eV than our calculated reaction barrier (0.86 eV) on pure Ni(1 1 1), which indicates that the incorporation of Co into the Ni crystal is not in favor of the reaction C + O, that is, O species from CO_2 dissociation can not eliminate the carbon deposition in CH_4/CO_2 reforming.

It is necessary to point out that our results are not in line with the above experimental results [12,13], suggesting that it is indispensable to consider other factors effect on reaction, e.g., strong metal–support interaction.

4. Conclusion

In this work, we conduct a DFT-based computational study on the adsorption of C, O and CO as well as C + O reaction on NiCo(1 1 1) bimetallic alloy model, and compare the results with that on pure Ni(1 1 1). DFT calculations show that the preferred site of C, O and CO on NiCo(1 1 1) is threefold sites like those on pure Ni(1 1 1). Strictly speaking, O and C prefer to bond with two Co atoms and one Ni atom at FCC-1 and HCP-1 site, respectively, while CO prefer to bond with two Ni atoms and one Co atom at HCP-2 site.

On the basis of the coadsorption of C and O, the association of C and O is investigated. The results show that the reation of C + O are exothermic, indicating favorable in thermodynamic. In dynamics, the favorable reaction path is that C adsorbed on HCP-1 site associates with O adsorbed on FCC-1 site resulting in CO adsorbed on bridge site of Ni–Co. However, the reaction barrier is higher by 0.35 eV than that on pure Ni(1 1 1), which indicates that the incorporation of Co into the Ni crystal is not in favor of carbon elimination.

Acknowledgements

The work was supported by the National Natural Science Foundation of China (Grant No. 20976115) and the National Younger Natural Science Foundation of China (Grant No. 20906066).

References

[1] K. Tomishige, Y.G. Chen, K. Fujimoto, J. Catal. 181 (1999) 91–103.
[2] J.R. Rostrup-Nielsen, J.H.B. Hansen, J. Catal. 144 (1993) 38–49.
[3] A. Erdöhelyi, J. Cserényi, F. Solymosi, J. Catal. 141 (1993) 287–299.
[4] O. Tokunaga, Y. Osada, S. Ogasawara, Fuel 68 (1989) 990–994.
[5] J.H. Kim, D.J. Suh, T.J. Park, K.L. Kim, Appl. Catal. A: Gen. 197 (2000) 191–200.
[6] R. Takahashi, S. Sato, T. Sodesawa, M. Kato, S. Takenaka, S. Yoshida, J. Catal. 204 (2001) 259–271.
[7] S. Tang, L. Ji, J. Lin, H.C. Zeng, K.L. Tan, K. Li, J. Catal. 194 (2000) 424–430.
[8] V.C.H. Kroll, H.M. Swaan, C. Mirodatos, J. Catal. 161 (1996) 409–422.
[9] H.M. Swaan, V.C.H. Kroll, G.A. Martin, C. Mirodatos, Catal. Today 21 (1994) 571–578.
[10] J.R. Rostrup-Nielsen, I. Alstrup, Catal. Today 53 (1999) 311–316.
[11] I. Alstrup, J.R. Rostrup-Nielsen, J. Catal. 100 (1986) 545–548.
[12] K. Takanabe, K. Nagaoka, K. Nariai, K. Aika, J. Catal. 232 (2005) 268–275.
[13] J. Zhang, H. Wang, A.K. Dalai, J. Catal. 249 (2007) 300–310.
[14] C.H. Bartholomew, Catal. Rev. Sci. Eng. 24 (1982) 67–112.
[15] F. Abild-Pedersen, J.K. Nørskov, J.R. Rostrup-Nielsen, J. Sehested, S. Helveg, Phys. Rev. B 73 (2006) 11541901–11541913.
[16] S.C. Tsang, J.B. Claridge, M.L.H. Green, Catal. Today 23 (1995) 3–15.
[17] J.M.H. Lo, T. Ziegler, J. Phys. Chem. C 112 (2008) 3679–3691.
[18] C.F. Huo, J. Ren, Y.W. Li, J. Wang, H. Jiao, J. Catal. 249 (2007) 174–184.
[19] Y. Morikawa, J.J. Mortensen, B. Hammer, J.K. Nørskov, Surf. Sci. 386 (1997) 67–72.
[20] T. Li, B. Bhatia, D.S. Sholl, J. Chem. Phys. 121 (2004) 10241–10249.
[21] M. Mavrikakis, M. Bäumer, H.J. Freund, J.K. Nørskov, Catal. Lett. 81 (2002) 153–156.
[22] M.P. Andersson, F. Abild-Pedersen, I.N. Remediakis, T. Bligaard, G. Jones, J. Engbæk, O. Lytken, S. Horch, J.H. Nielsen, J. Sehested, J.R. Rostrup-Nielsen, I. Nørskov, Chorkendorff, J. Catal. 255 (2008) 6–19.
[23] A. Michaelides, P. Hu, J. Chem. Phys. 114 (2001) 5792–5795.
[24] A.A. List, J.M. Blakely, Surf. Sci. 152/153 (1985) 463–470.
[25] M.C. Payne, D.C. Allan, T.A. Arias, J.D. Joannopoulos, Rev. Mod. Phys. 64 (1992) 1045–1097.
[26] V. Milman, B. Winkler, J.A. White, C.J. Pickard, M.C. Payne, E.V. Akhmatsakaya, R.H. Nobes, Int. J. Quantum Chem. 77 (2000) 895–910.
[27] J.P. Perdew, K. Burke, M. Ernzerhof, Phys. Rev. Lett. 77 (1996) 3865–3868.
[28] D. Vanderbilt, Phys. Rev. B 41 (1990) 7892–7895.
[29] H.J. Monkhorst, J.D. Pack, Phys. Rev. B 13 (1976) 5188–5192.
[30] V. Shah, T. Li, K.L. Baumert, H. Cheng, D.S. Sholl, Surf. Sci. 527 (2003) 217–227.
[31] S.G. Wang, X.Y. Liao, J. Hu, D.B. Cao, Y.W. Li, J. Wang, H. Jiao, Surf. Sci. 601 (2007) 1271–1284.
[32] T.A. Halgren, W.N. Lipscomb, Chem. Phys. Lett. 49 (1977) 225–232.
[33] H. Liu, R. Zhang, R. Yan, B. Wang, K. Xie, Appl. Sur. Sci. (2011), doi:10.1016/j.apsusc.2011.05.073.